October 30, 2000

RIA Application Workshop 2000

Los Alamos National Laboratory, October 30-31, 2000

Stepan MASHNIK

T-16, Theoretical Division
Los Alamos National Laboratory
Los Alamos, NM, 87545

RIA potential for improving models for ATW calculations

Nuclear Data Evaluation for Accelerator-Driven Systems

Kalmar '96

Arjan Koning
ECN Nuclear Energy, Netherlands Energy Research Foundation ECN,
P.O. Box 1, 1755 ZG Petten, The Netherlands

Element	Quantity	Energy (MeV)	Accuracy(%)	Application/Comments
C	(n,xn)*,(n,γ),(n,xp)...(n,xα)	20-250	20	Medical purposes, ADS
	(p,el),(p,reac),	0-250	5-10	
	(p,xn)†,(p,xp)†,(p,γ),(p,xd)...(p,xα)		30	
N	(p,xn),(p,xp),(n,xn),(n,xp)	20-1500	50	ADS
O	(n,xn)*,(n,γ),(n,xp)...(n,xα)	20-250	20	Medical purposes, ADS
	(p,el),(p,reac),	0-250	5-10	
	(p,xn)†,(p,xp)†,(p,γ),(p,xd)...(p,xα)		30	
Na	(p,xn),(p,xp),(n,xn),(n,xp)	20-1500	50	ADS
Al	(n,xn)*,(n,γ),[redacted]	20-200	5-10	ADS, fusion (up to 50 MeV),
	(n,xp)...(n,xα)		20	structural material, shielding,
	(p,el),(p,reac),(p,p')	0-250	5-10	transport calculations
	(p,xn)†,(p,xp)†,[redacted],(p,xd)...(p,xα)		30	
Cl	(p,xn),(p,xp),(n,xn),(n,xp)	20-1500	50	ADS
Fe	(n,xn)*,(n,γ),p.c.s.	20-200	5-10	ADS, fusion (up to 50 MeV),
	(n,xp)...(n,xα)		20	structural material, shielding,
	(p,el),(p,reac),(p,p')	0-250	5-10	transport calculations
	(p,xn)†,(p,xp)†,[redacted],(p,xd)...(p,xα)		30	
Cu	(p,xn),(p,xp),(n,xn),(n,xp)	20-1500	50	ADS
Zr	(p,xn)‡,(p,xp)‡,[redacted]	0-1500	30	ADS, shielding/transport calc.
	(p,xd)...(p,xα)		30	(p,xp) for model validation.
Nb	(p,xn),(p,xp),(n,xn),(n,xp)	20-1500	50	ADS
Mo	(p,xn),(p,xp),(n,xn),(n,xp)	20-1500	50	ADS
Tc	(p,xn),(p,xp),(n,xn),(n,xp)	20-1500	50	ADS
I	(p,xn),(p,xp),(n,xn),(n,xp)	20-1500	50	ADS
Ta	(p,xn),(p,xp),(n,xn),(n,xp)	20-1500	50	ADS
W	(n,xn),(n,xγ),[redacted]	20-200	30	ADS, target material,
	(n,xp)...(n,xα)		30	
	(p,xn)‡,(p,xp)*,[redacted],(p,xd)...(p,xα)	0-1500	30	transport calculations
Hg	(p,xn),(p,xp),(n,xn),(n,xp)	20-1500	50	ADS
Pb	(n,xn),(n,xγ),p.c.s.,(n,xp)...(n,xα)	20-200	30	ADS, target material,
	(p,xn)‡,(p,xp)*,[redacted]	0-1500	30	transport calculations
	(p,xd)...(p,xα),(p,f)		30	(p,xp) for model validation
Bi	(p,xn),(p,xp),(n,xn),(n,xp)	20-1500	50	ADS
Th	(n,tot),(n,el),(n,n')	0-200	5-10	ADS, actinide, transport calc.,
	(n,xn)*,(n,γ)		20	NEA Pilot Evaluation
	(n,xp),...(n,xα),(n,f)		30	
Np	(p,xn),(p,xp),(n,xn),(n,xp)	20-1500	50	ADS
Pu	(p,xn),(p,xp),(n,xn),(n,xp)	20-1500	50	ADS
Am	(p,xn),(p,xp),(n,xn),(n,xp)	20-1500	50	ADS
Cm	(p,xn),(p,xp),(n,xn),(n,xp)	20-1500	50	ADS

ADS: Accelerator-driven systems, p.c.s.: Production cross sections

* Recommended energies for measurements: 25, 45, 80, (120, 160, 256, 800) MeV.

† Recommended energies for measurements: 25, (65) MeV.

‡ Energies above 800 MeV only.

Note: At some energies the requests could have been met by recent measurements. All elements with an accuracy of 50% for energies between 20-1500 MeV are from a recent Japanese high-priority list. More specification is still required.

Figure 1: High-priority nuclear data request list for intermediate energies

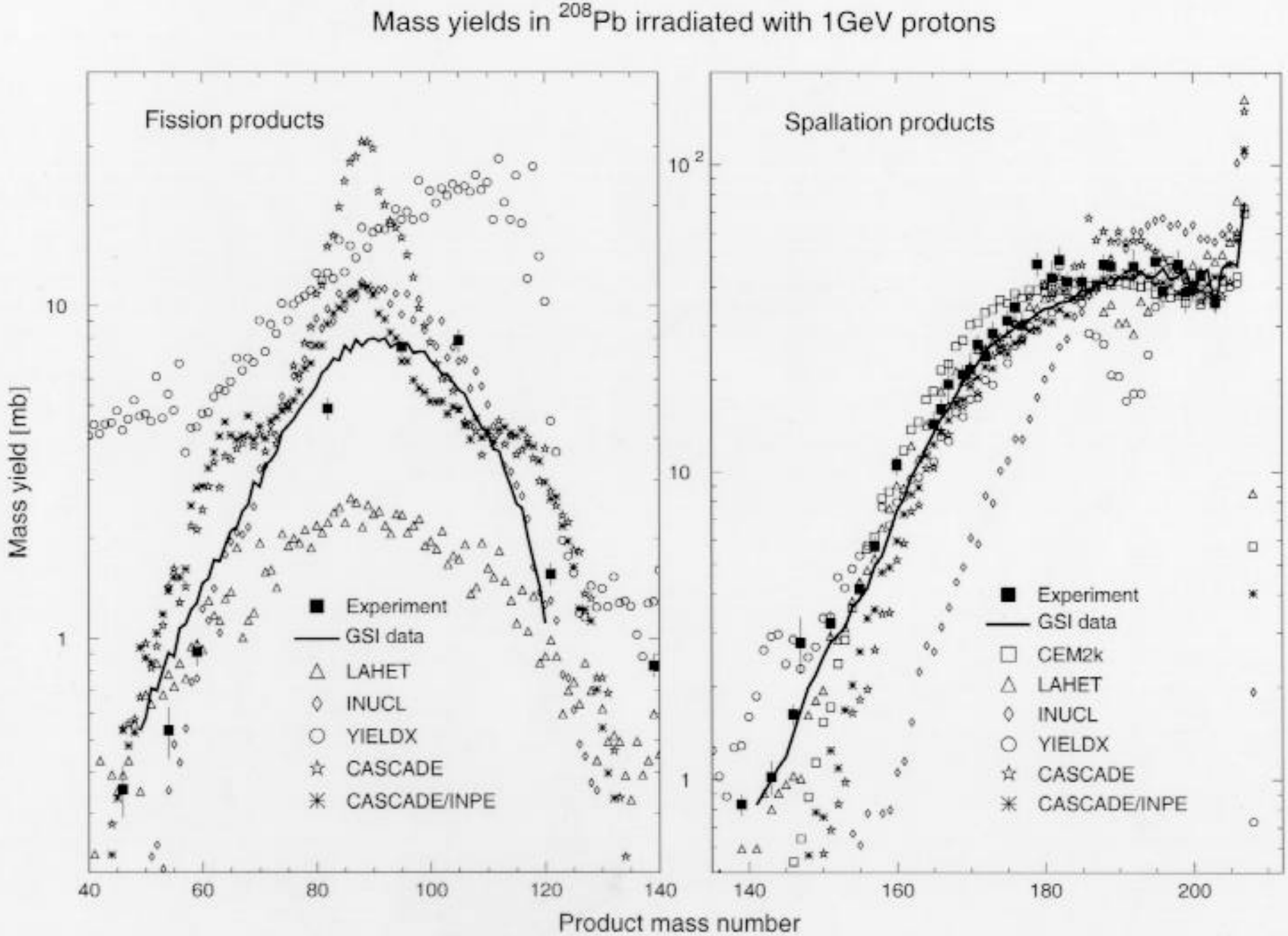
Mass yields in 208Pb irradiated with 1GeV protons
Fission products
Spallation products
Mass yield [mb]
Product mass number
Experiment
GSI data
LAHET
INUCL
YIELDX
CASCADE
CASCADE/INPE
CEM2k
10
1
10 2
40
60
80
100
120
140
160
180
200

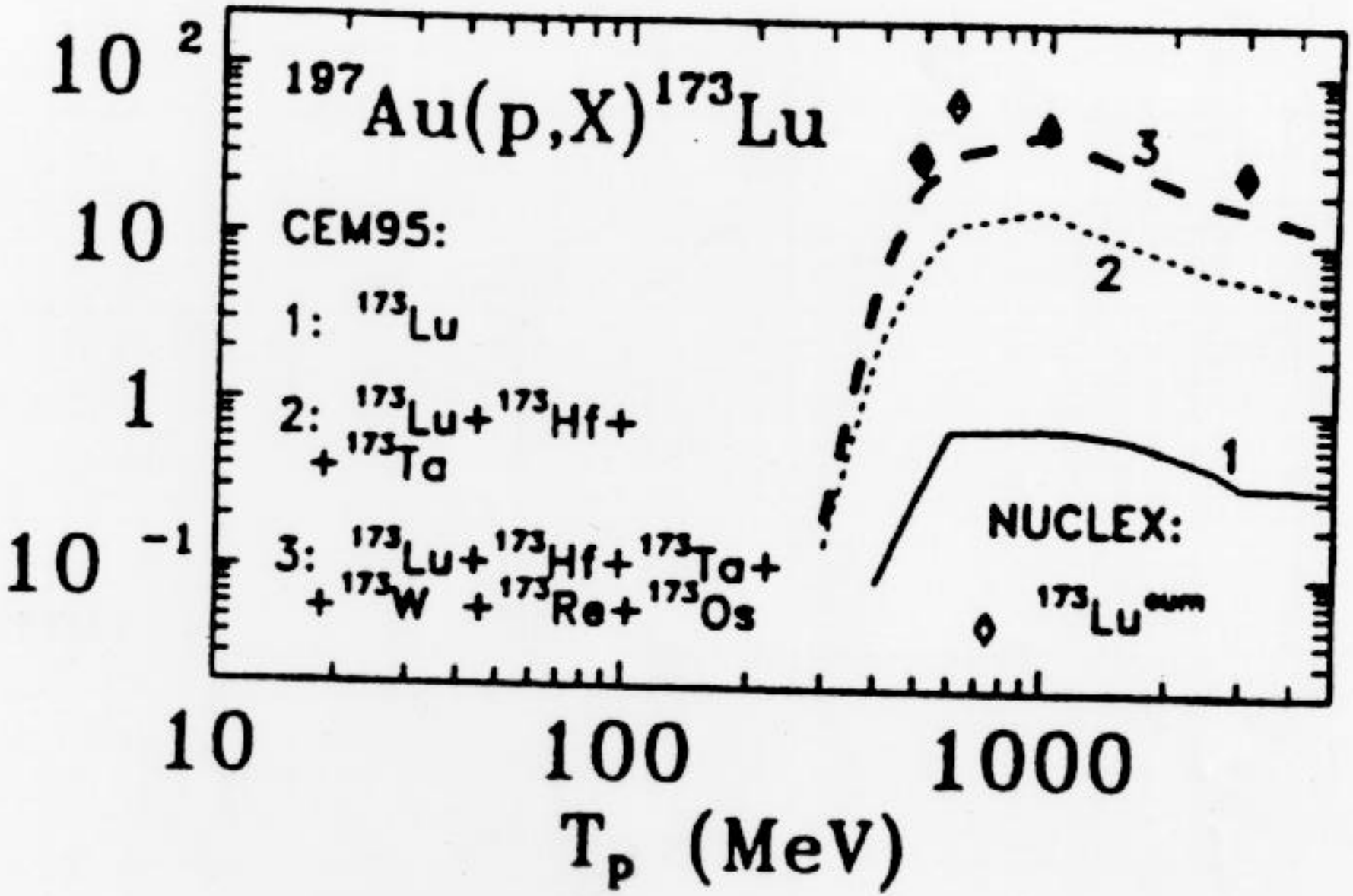
$^{197}Au(p,X)^{173}Lu$
CEM95:
1: ^{173}Lu
2: $^{173}Lu + ^{173}Hf + ^{173}Ta$
3: $^{173}Lu + ^{173}Hf + ^{173}Ta + ^{173}W + ^{173}Re + ^{173}Os$
NUCLEX:
$^{173}Lu^{sum}$
1
2
3
10^{2}
10
1
10^{-1}
10
100
1000
T_p (MeV)

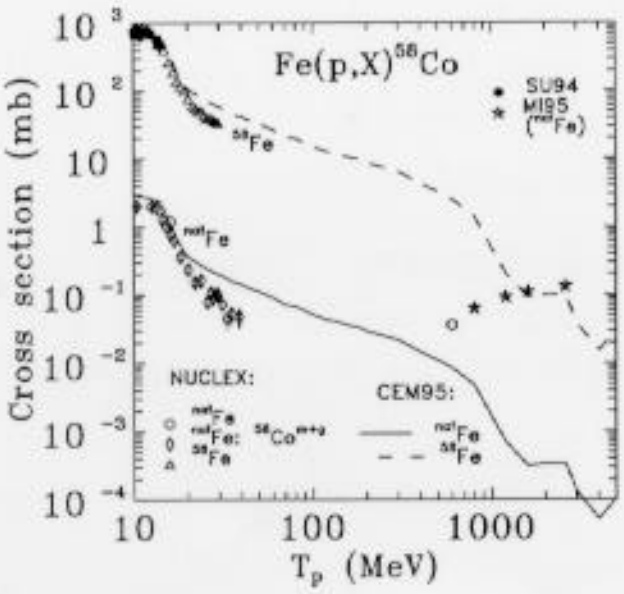
Fe(p,X)56Co
SU94
MI95
(natFe)
56Fe
natFe
NUCLEX:
natFe
natFe: 56Co m+g
56Fe
CEM95:
natFe
56Fe
Cross section (mb)
Tp (MeV)

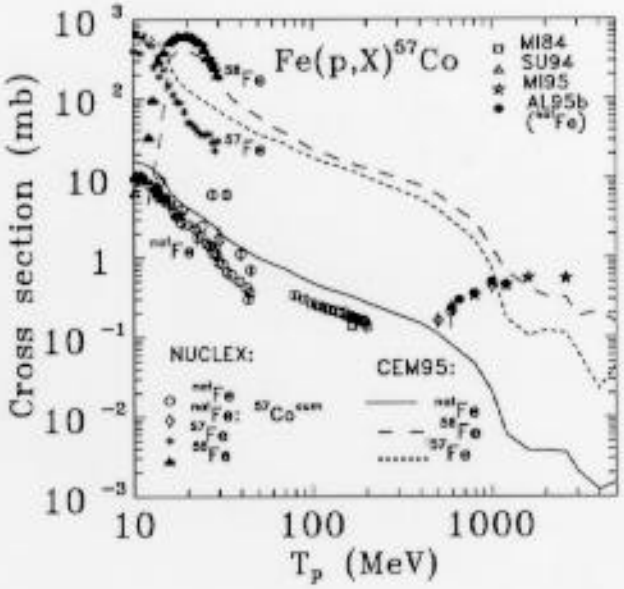
Fe(p,X)57Co
MI84
SU94
MI95
AL95b
(natFe)
56Fe
57Fe
natFe
NUCLEX:
natFe
natFe: 57Co sum
57Fe
56Fe
CEM95:
natFe
56Fe
57Fe
Cross section (mb)
Tp (MeV)

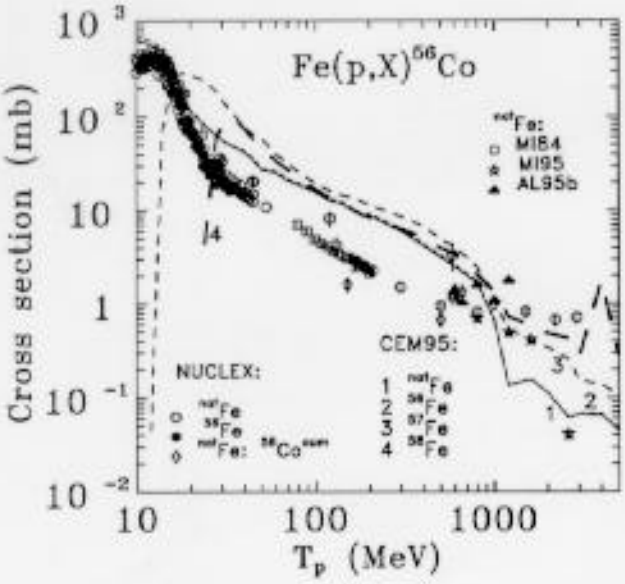
Fe(p,X)56Co
natFe:
MI84
MI95
AL95b
NUCLEX:
natFe
56Fe
natFe: 56Co sum
CEM95:
1 natFe
2 56Fe
3 57Fe
4 56Fe
Cross section (mb)
Tp (MeV)

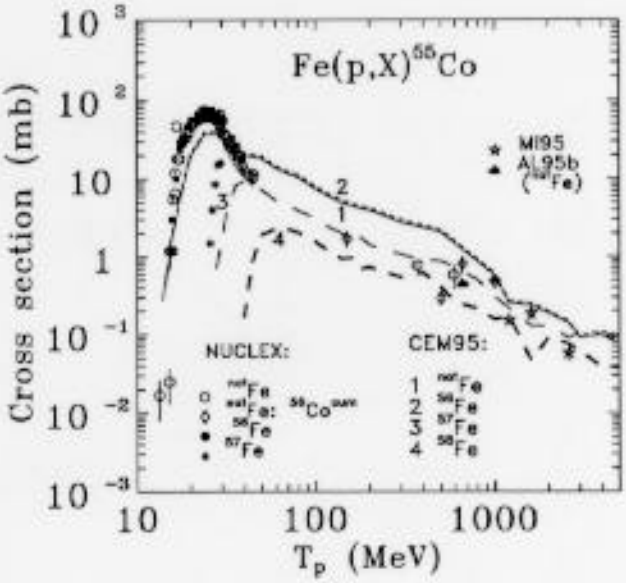
Fe(p,X)55Co
MI95
AL95b
(natFe)
NUCLEX:
natFe
natFe: 55Co sum
56Fe
57Fe
CEM95:
1 natFe
2 56Fe
3 57Fe
4 56Fe
Cross section (mb)
Tp (MeV)

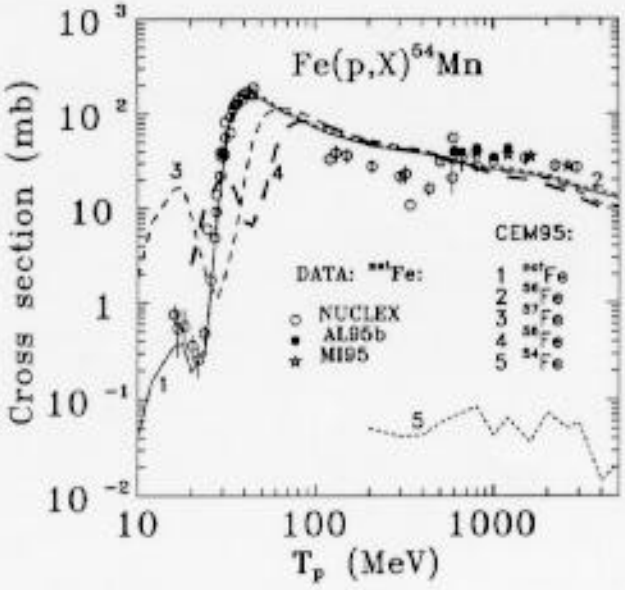
Fe(p,X)54Mn
DATA: natFe:
NUCLEX
AL95b
MI95
CEM95:
1 natFe
2 56Fe
3 57Fe
4 56Fe
5 54Fe
Cross section (mb)
Tp (MeV)

Cross Sections of Spallation Residues Produced in 1A GeV ^{208}Pb on Proton Reactions

W. Wlazło,[1,6] T. Enqvist,[2,*] P. Armbruster,[2] J. Benlliure,[2,3] M. Bernas,[4] A. Boudard,[1] S. Czájkowski,[5] R. Legrain,[1] S. Leray,[1] B. Mustapha,[4] M. Pravikoff,[5] F. Rejmund,[2,4] K.-H. Schmidt,[2] C. Stéphan,[4] J. Taieb,[2,4] L. Tassan-Got,[4] and C. Volant[1]

[1]*DAPNIA/SPhN CEA/Saclay, F-91191 Gif-sur-Yvette Cedex, France*
[2]*GSI, Planckstrasse 1, D-64291 Darmstadt, Germany*
[3]*University of Santiago de Compostela, 15706 Santiago de Compostela, Spain*
[4]*IPN Orsay, BP1, F-91406 Orsay Cedex, France*
[5]*CEN Bordeaux-Gradignan, F-33175, Gradignan, France*
[6]*Jagiellonian University, Institute of Physics, ulica Reymonta 4, 30-059 Kraków, Poland*
(Received 11 February 2000)

Spallation residues produced in 1 GeV per nucleon ^{208}Pb on proton reactions have been studied using the Fragment Separator facility at GSI. Isotopic production cross sections of elements from $_{61}$Pm to $_{82}$Pb have been measured down to 0.1 mb with a high accuracy. The recoil kinetic energies of the produced fragments were also determined. The obtained cross sections agree with most of the few existing gamma-spectroscopic data. The data are compared with different intranuclear-cascade and evaporation-fission models. Drastic deviations were found for a standard code used in technical applications.

PACS numbers: 25.40.Sc, 24.10.−i, 25.70.Mn, 29.25.Dz

Spallation reactions have recently captured an increasing interest due to their technical applications as intense neutron sources for accelerator-driven subcritical reactors [1] or spallation neutron sources [2]. The design of an accelerator-driven system (ADS) requires precise knowledge of nuclide production cross sections in order to be able to predict the amount of radioactive isotopes produced inside the spallation target. Indeed, short-lived isotopes may be responsible for maintenance problems and long-lived ones will increase the long term radiotoxicity of the system. Recoil kinetic energies of the fragments are important for studies of radiation damages in the structure materials or in the case of a solid target. Data concerning lead are particularly important since in most of the ADS concepts actually discussed, lead or lead-bismuth alloy is considered as the preferred material of the spallation target.

The present experiment, using inverse kinematics, is able to supply the identification of all the isotopes produced in spallation reactions and information on their recoil velocity. Moreover, the data represent a crucial benchmark for the existing spallation models used in the ADS technology. The precision of these models to estimate residue production cross sections is still far from the performance required for technical applications, as it was shown in Ref. [3]. This can be mostly ascribed to the lack of complete distributions of all produced isotopes to constrain the models. The available data were generally obtained by chemistry or gamma spectroscopy [4–6] which give access mostly to cumulative yields produced after long chains of decaying isotopes.

In this Letter, we report on complete isotopical production cross sections for heavy fragments produced in spallation of ^{208}Pb on proton at 1A GeV, down to 0.1 mb with a high precision. The kinematic properties of the residues are also studied. The cross sections of lighter isotopes produced by fission will be presented in a forthcoming publication.

The experimental method and the analysis procedure have been developed and applied in previous experiments [7–9]. The primary beam of 1A GeV ^{208}Pb was delivered by the heavy-ion synchrotron SIS at GSI, Darmstadt. The proton target was composed of 87.3 mg/cm^2 liquid hydrogen [10] enclosed between thin titanium foils of a total thickness of 36 mg/cm^2. The primary-beam intensity was continuously monitored by a beam-intensity monitor (SEETRAM) based on secondary-electron emission. In order to subtract the contribution of the target windows from the measured reaction rate, measurements were repeated with the empty target. Heavy residues produced in the target were all strongly forward focused due to the inverse reaction kinematics. They were identified using the Fragment Separator (FRS) [11].

The FRS is a two-stage magnetic spectrometer with a dispersive intermediate image plane (S_2) and an achromatic final image plane (S_4) with momentum acceptance of 3% and angular acceptance of 14.4 mrad around the beam axis. Two position-sensitive plastic scintillators placed at S_2 and S_4, respectively, provided the magnetic-rigidity ($B\rho$) and time-of-flight measurements, which allowed to determine the mass-over-charge ratio of the particles. In the analysis, totally stripped residues were considered only. In the case of residues with the highest nuclear charges (above $_{65}$Tb) an achromatic degrader (5.3 to 5.9 g/cm^2 of aluminum) was placed at S_2 to obtain a better Z resolution. The elements below terbium were identified from an energy-loss measurement in an ionization chamber (MUSIC). The velocity of the identified residue was determined at S_2 from the $B\rho$ value and transformed into the frame of the beam in the middle of the target taking into account the appropriate energy loss. About 100

 0031-9007/00/84(25)/5736(4)$15.00 © 2000 The American Physical Society

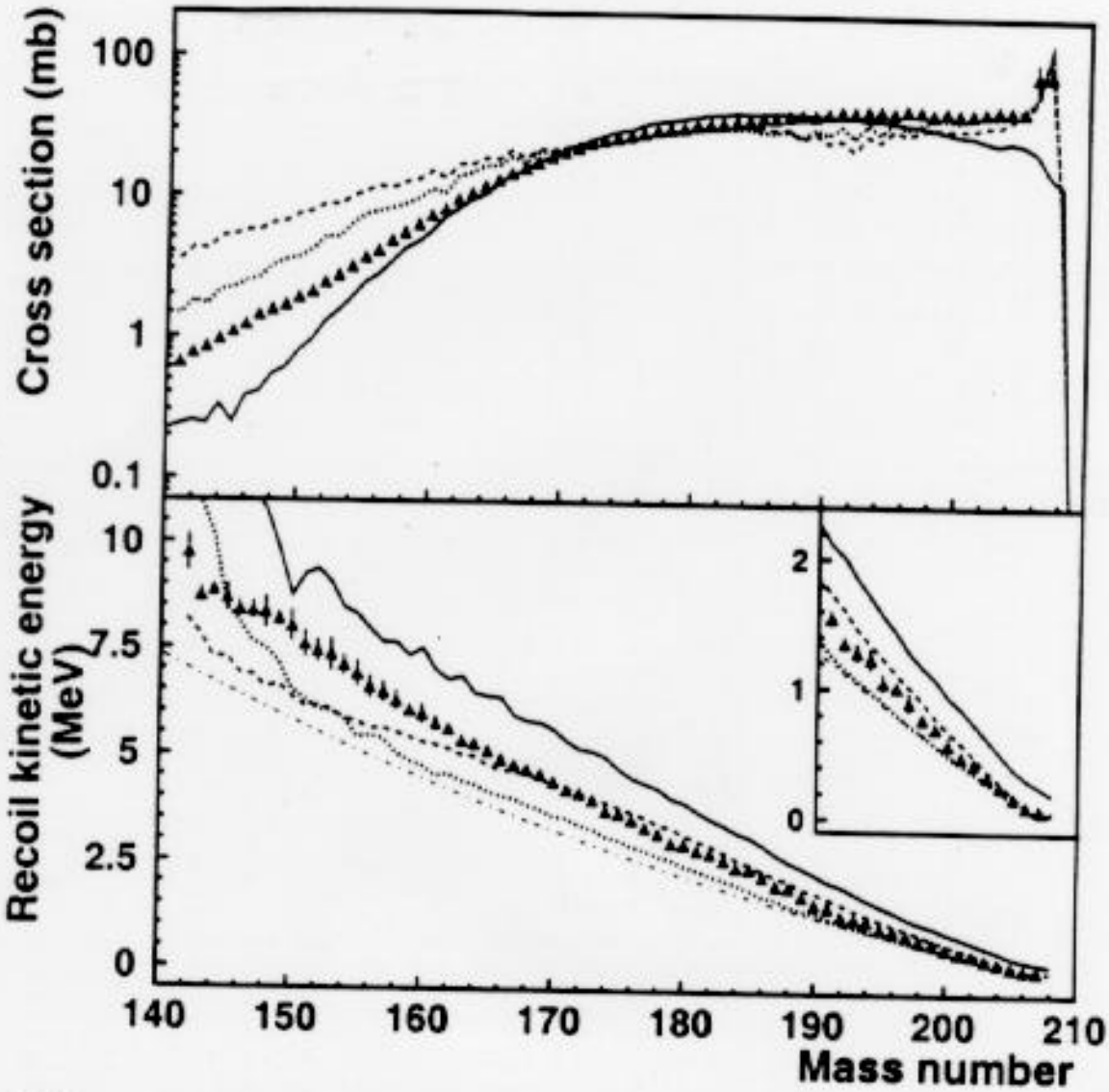

FIG. 3. Mass distribution (upper panel) and recoil kinetic energy (bottom panel) of the residues produced in 1·A GeV ^{208}Pb on hydrogen reactions (triangles) versus mass number, compared with the Cugnon-Schmidt (solid line), Bertini-Dresner (dashed line) and Isabel-Dresner (dotted line) models. The dash-dotted line shows the recoil kinetic energies expected from the Morrissey systematics [23].

The velocity distribution of each residue was also determined, from which it was possible to infer information about the recoil kinetic energy in the projectile sys-

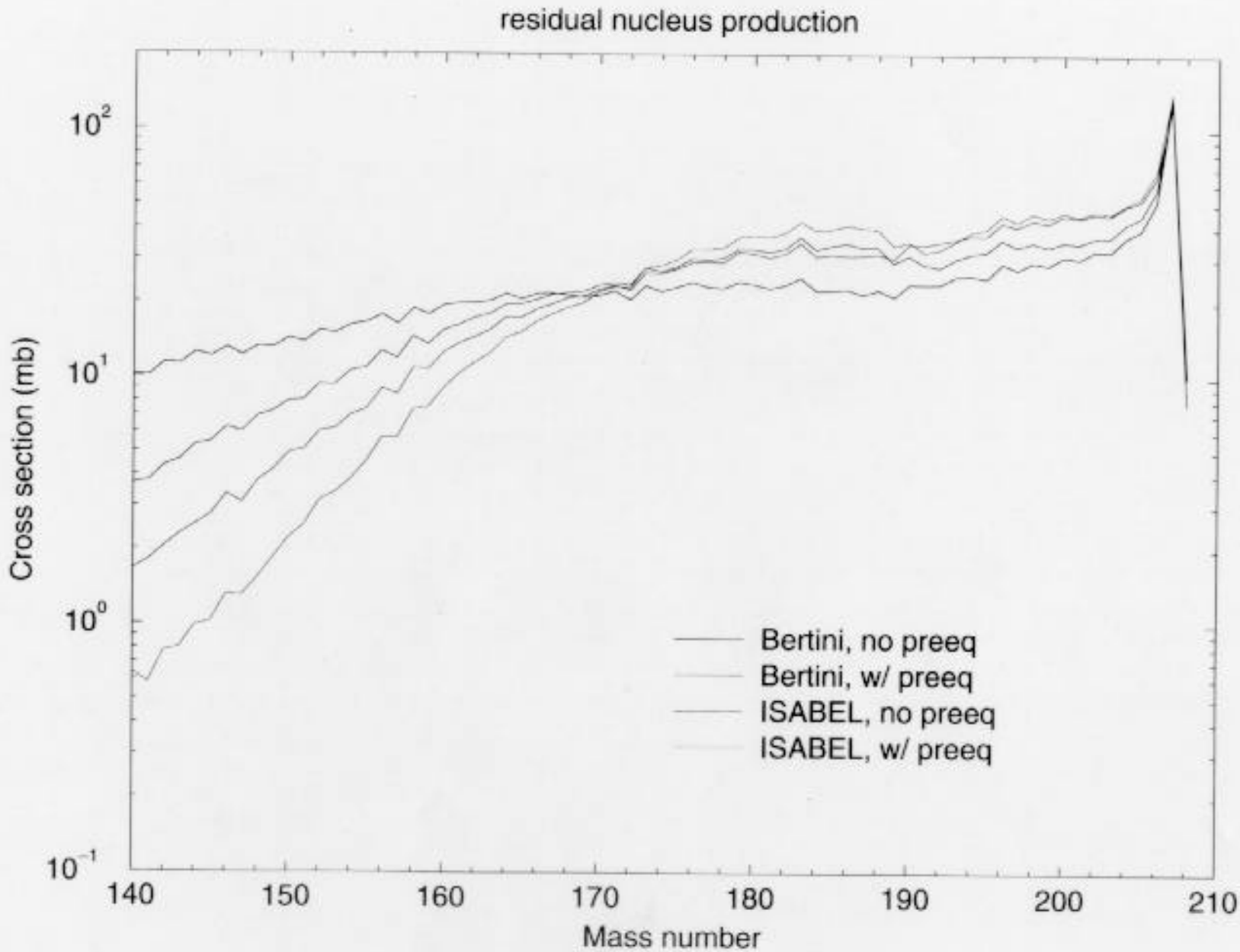
1 GeV p on Pb208
residual nucleus production
Cross section (mb)
10^2
10^1
10^0
10^{-1}
140
150
160
170
180
190
200
210
Mass number
Bertini, no preeq
Bertini, w/ preeq
ISABEL, no preeq
ISABEL, w/ preeq

2000/06/30 15.37

Mass yields in Pb-208 irradiated with 1GeV protons

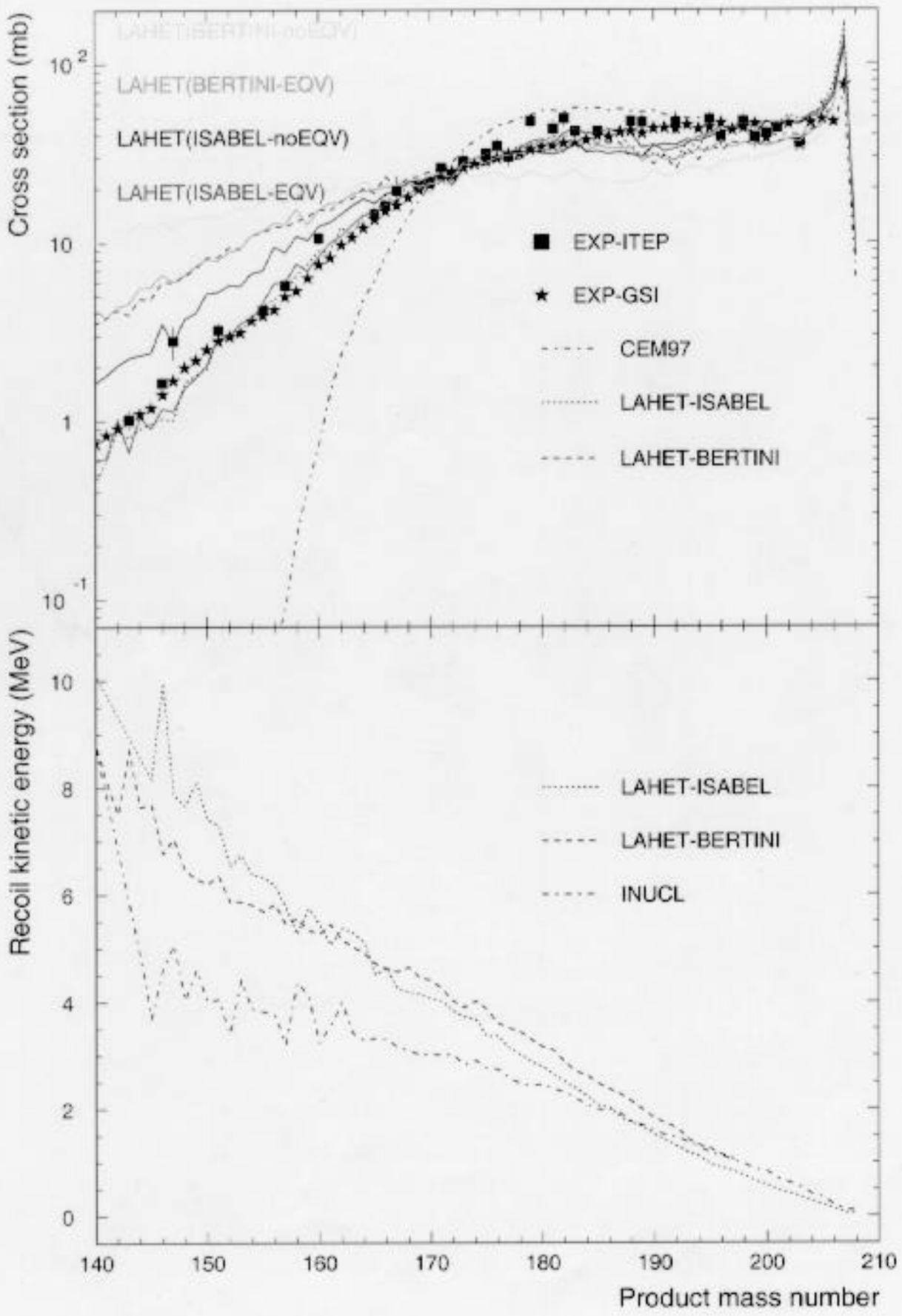

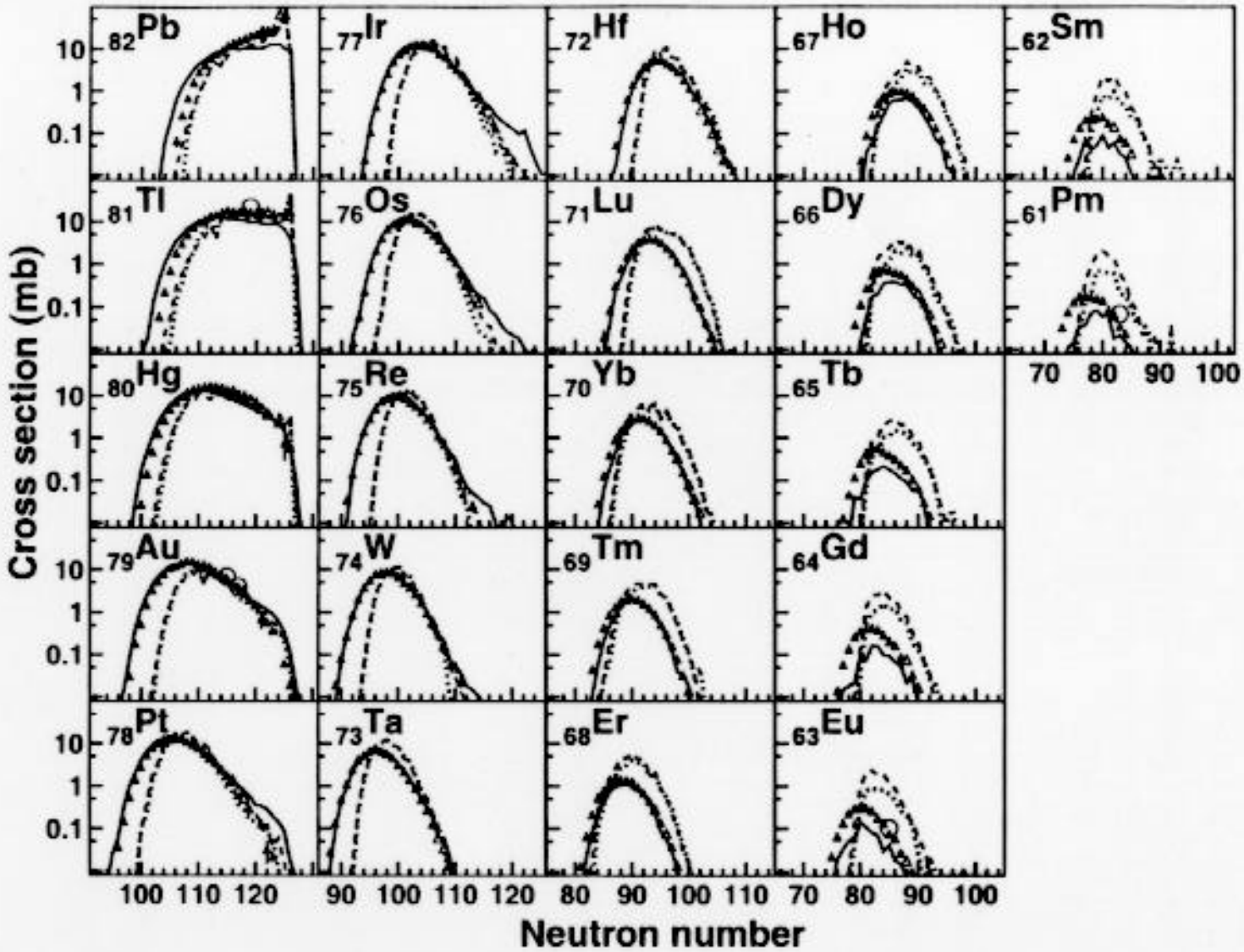

FIG. 2. Isotopic production cross-sections of elements between Z=82 and 61, in the reaction of 1·A GeV ^{208}Pb on hydroge versus neutron number. Stable (resp. radioactive) isotopes are marked by open (resp. full) triangles. Gamma-spectrosco data regarding shielded isotopes from [6] are plotted as open circles. The solid, dashed and dotted curves were calculated wi the Cugnon-Schmidt [20,21], Bertini [16]-Dresner [18,19] and Isabel [17]-Dresner models, respectively.

cross-section is the sum of the production of the ground and the isomeric states. The data agree within their error bars, except for the isotope with the lowest cross-section

to the fact that the prediction of the neutron-proto evaporation competition in the Dresner code is not sa

Isotopic distributions of the products in Pb-208+1GeV protons: GSI+LAHET-ISABE

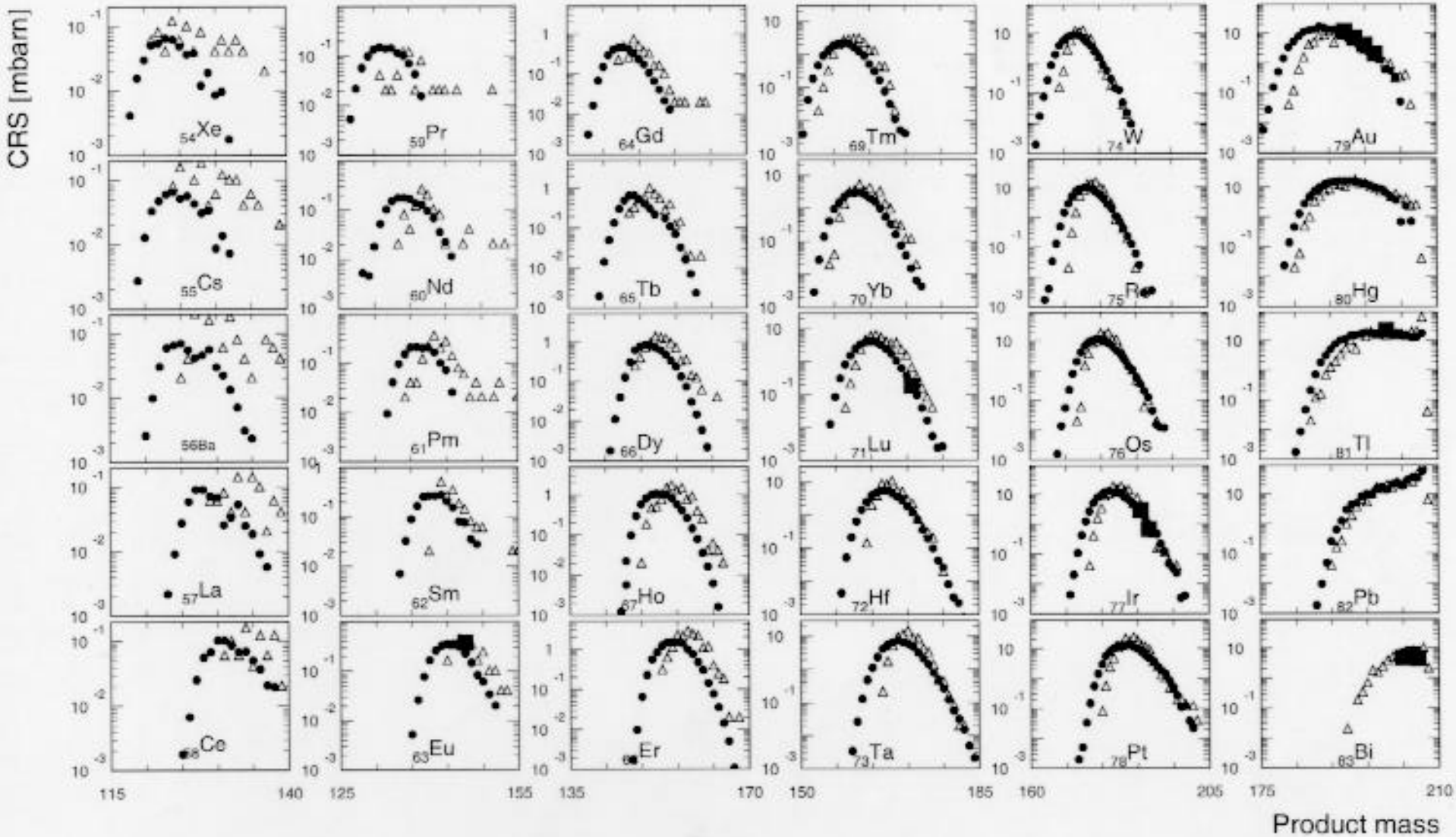

Isotopic distributions of the products in Pb-208+1GeV protons: GSI+LAHET-BERTIN

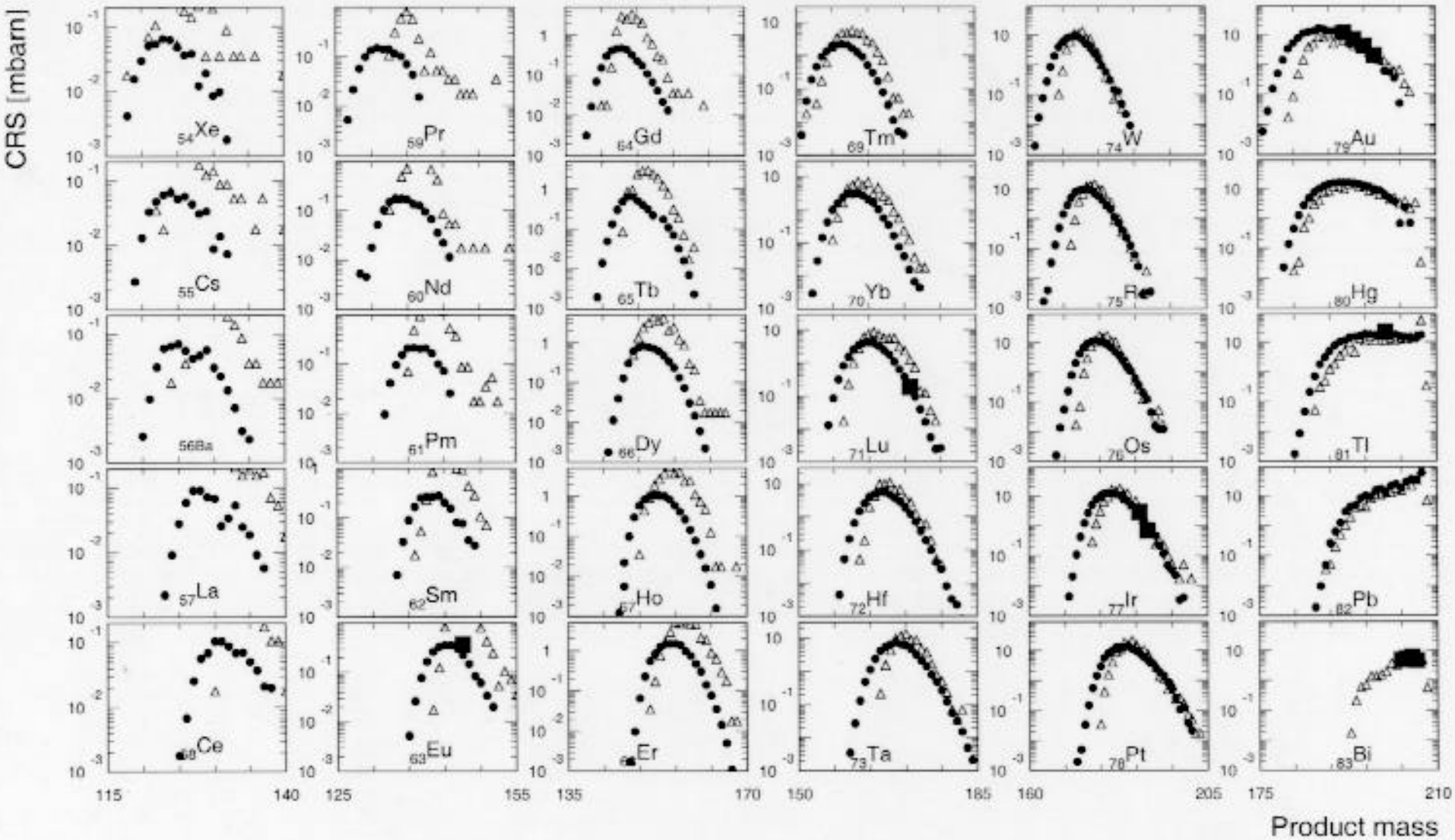

Isotopic distributions of the products in Pb-208+1GeV protons: GSI+YIELDX

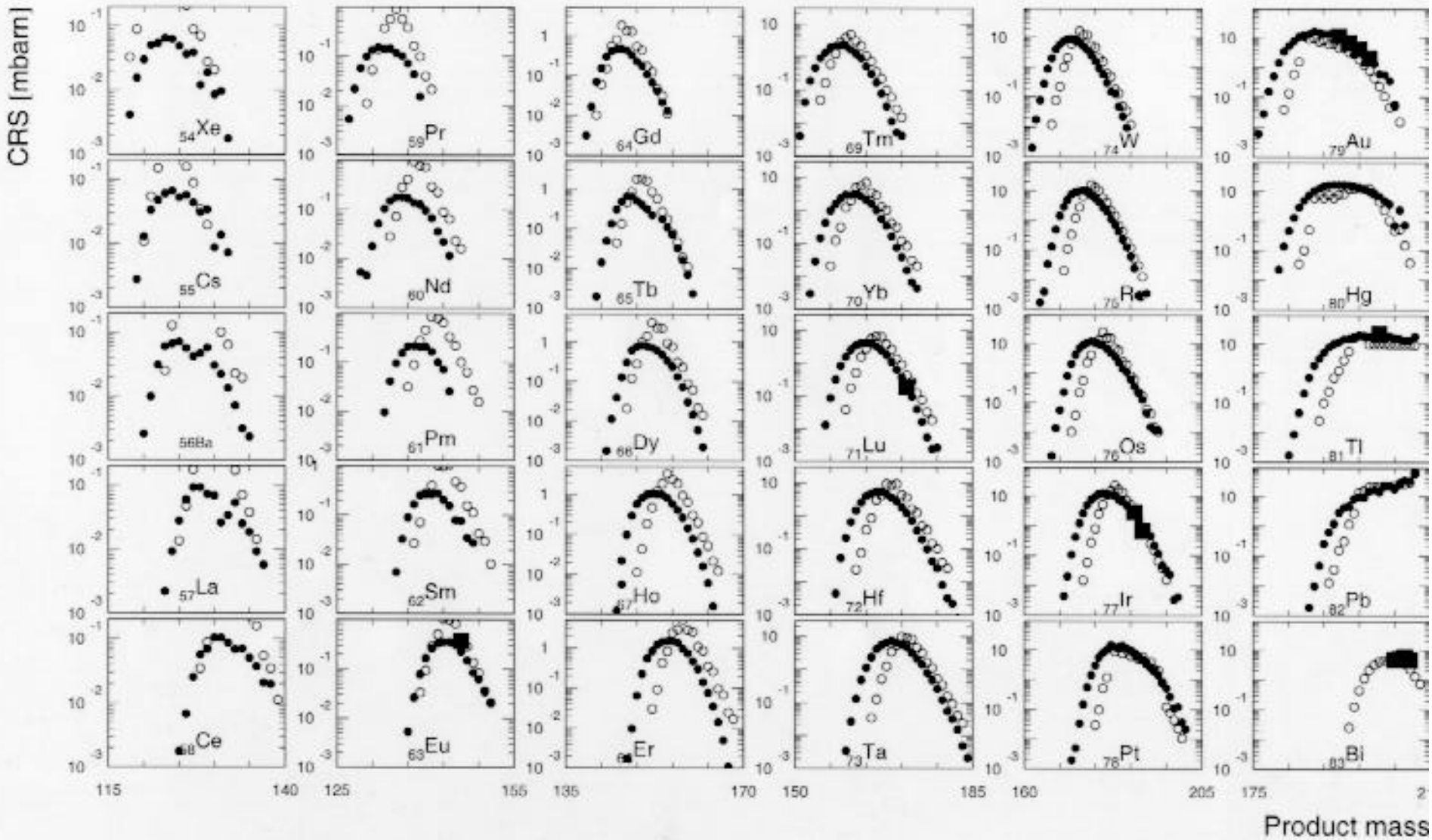

Isotopic distributions of the products in Pb-208+1GeV protons: GSI+INUCL

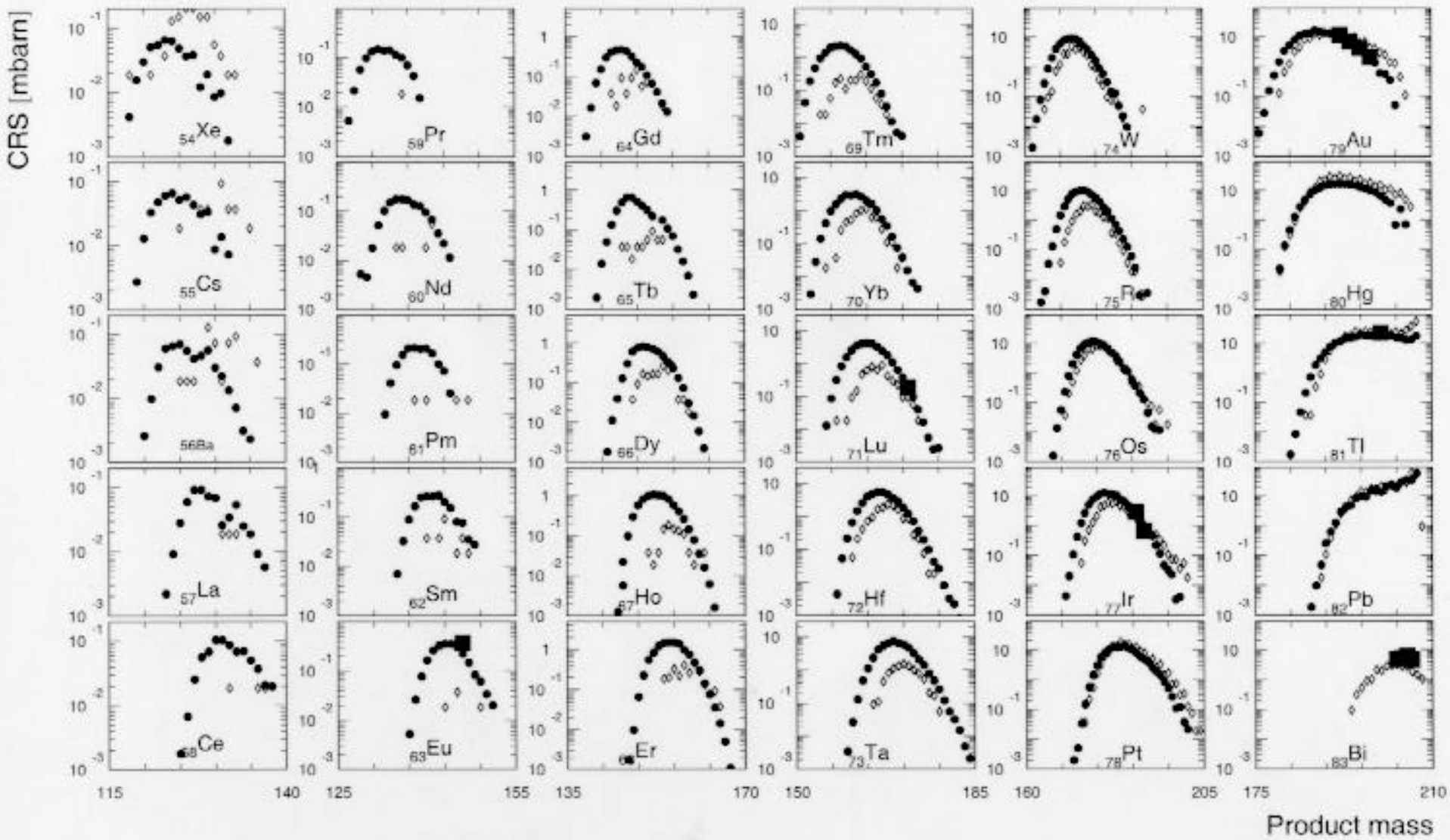

Isotopic distributions of the products in Pb-208+1GeV protons: GSI+CASCADE/INI

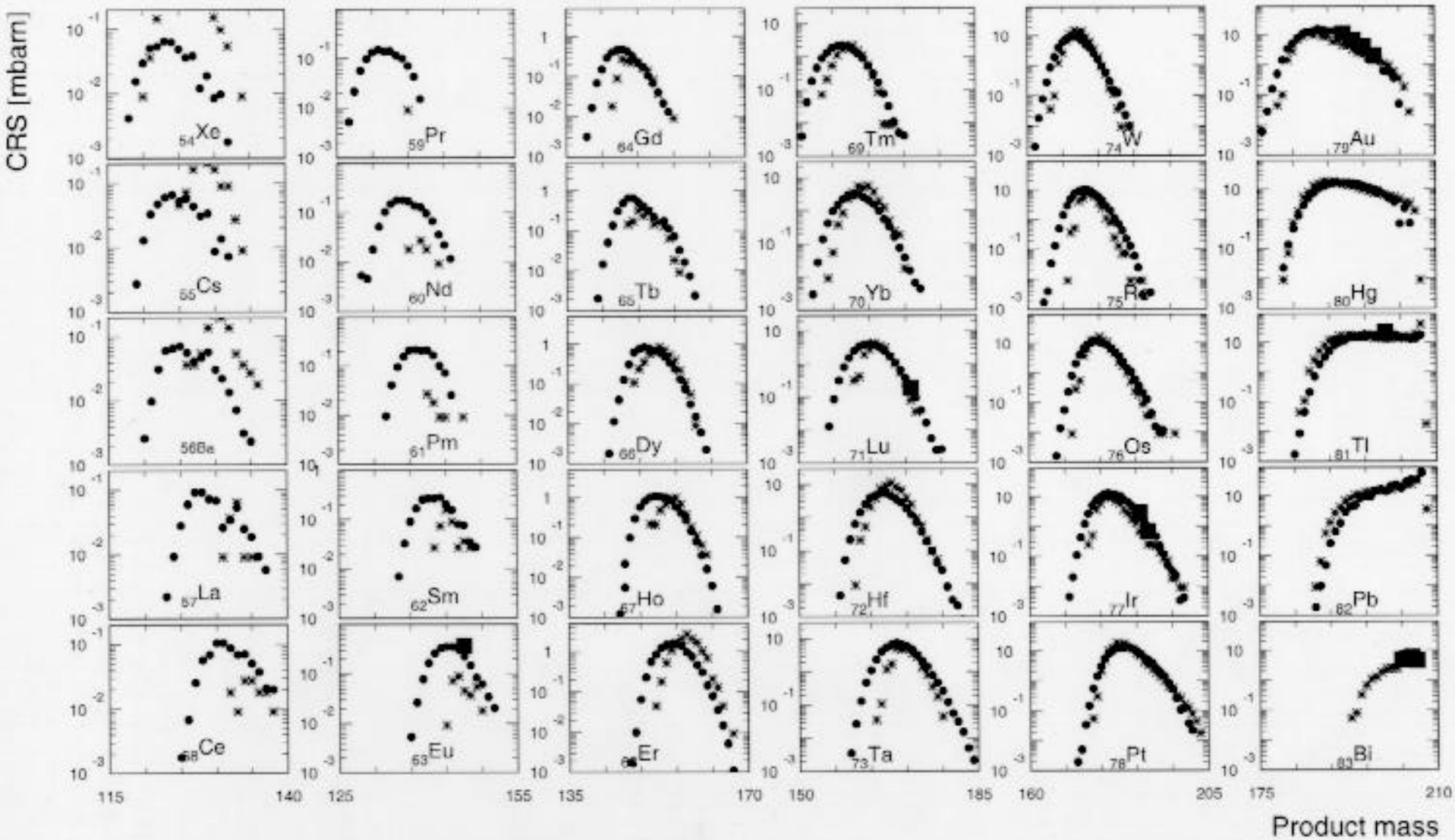

Isotopic distributions of the products in Pb-208+1GeV protons: GSI+CASCADE

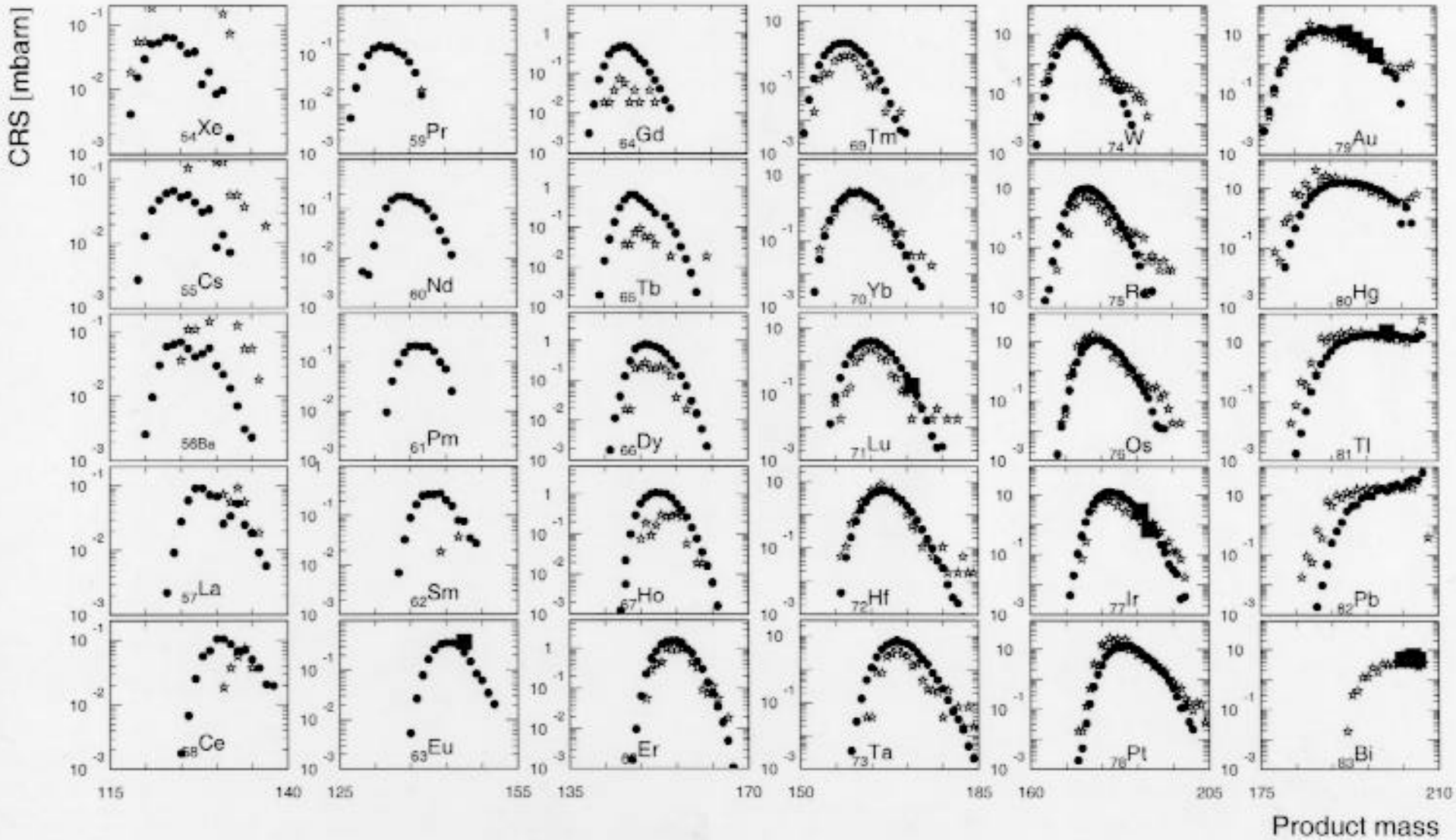

Isotopic distributions of the products in Pb-208+1GeV protons: GSI+ITEP+Codes

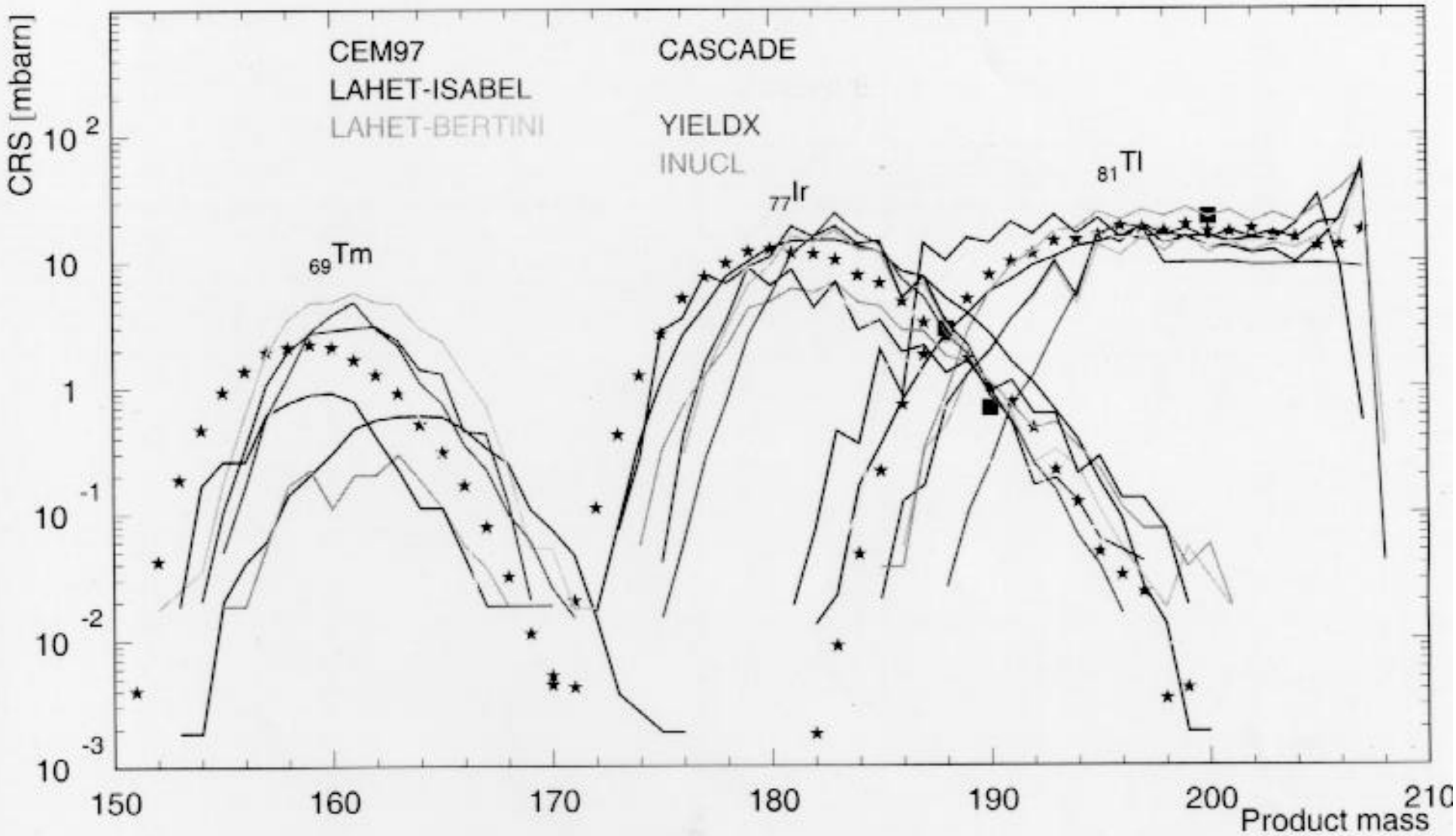

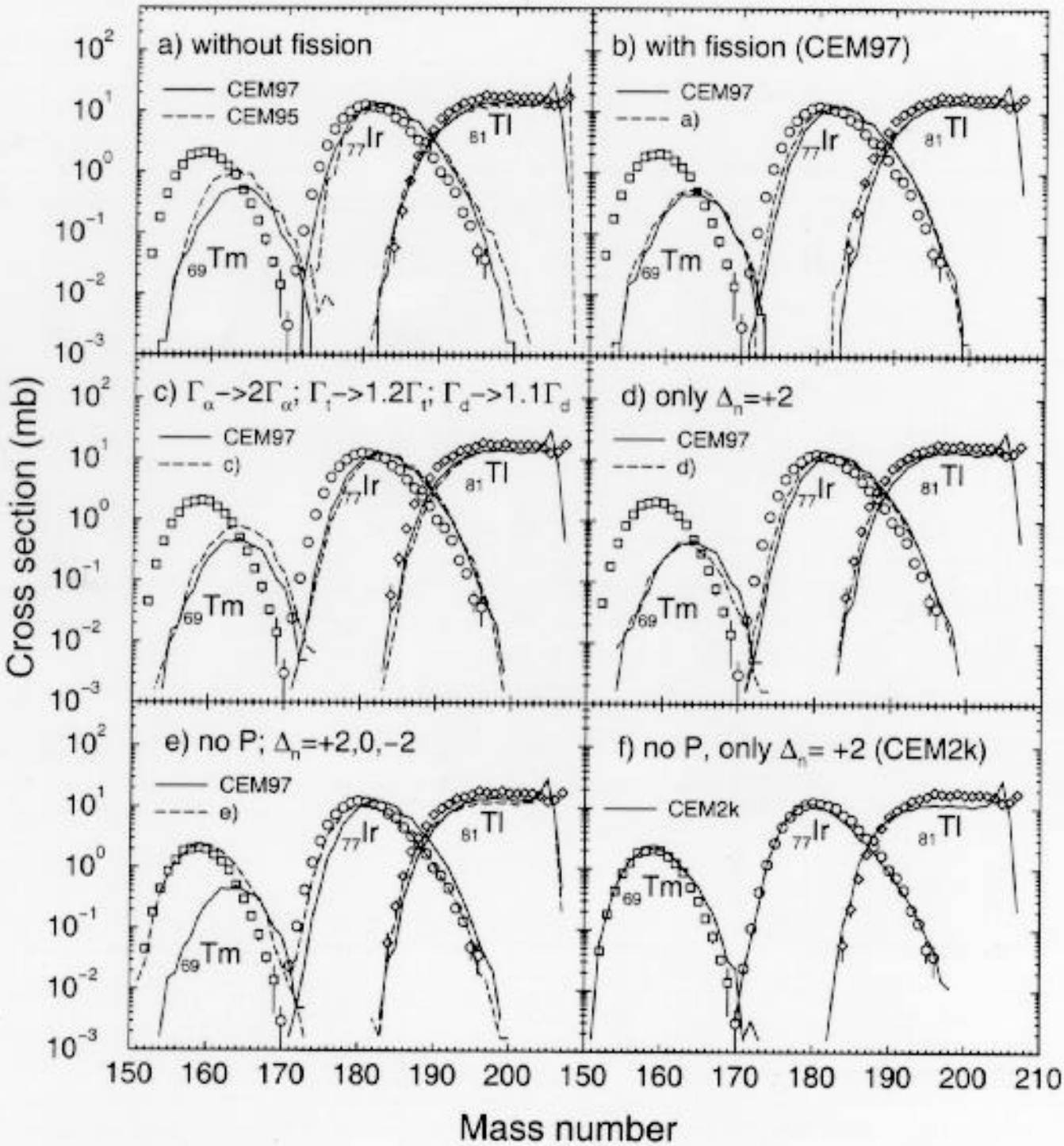

Figure 2: Example of several steps from CEM97 to CEM2k in analyzing production of ^{81}Tl, ^{77}Ir, and ^{69}Tm isotopes from ^{208}Pb interactions with liquid ^{1}H at 1 GeV/nucleon measured at GSI [3] (see details in the text).

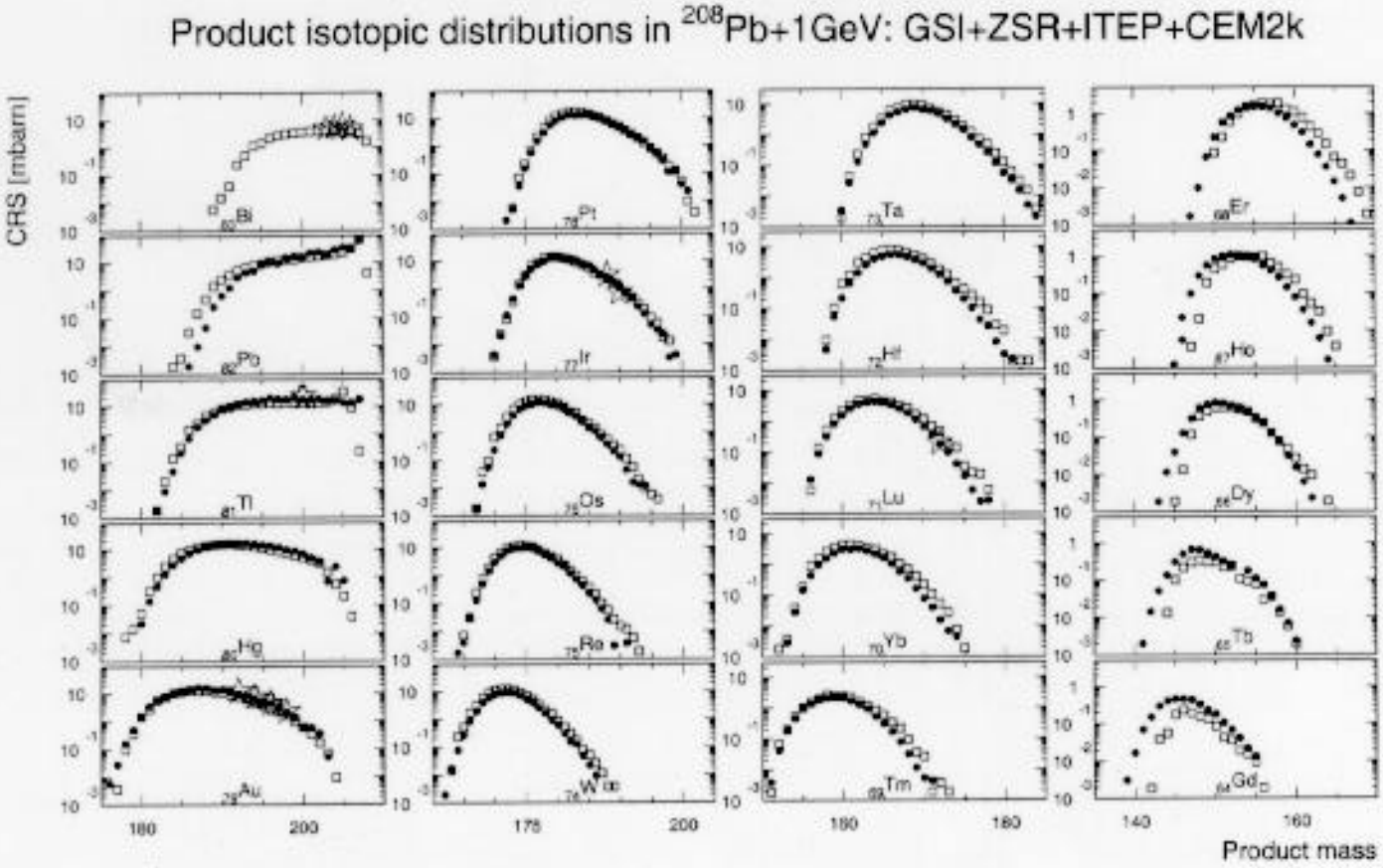

Figure 3: Isotopic production cross sections of elements between Z=64 and 83 in reaction of ^{208}Pb on hydrogen at 1 GeV/n. Filled circles show GSI data [6], opened stars are recent ITEP data measured by the γ-spectromerty method [16], opened squares show present CEM2k results.

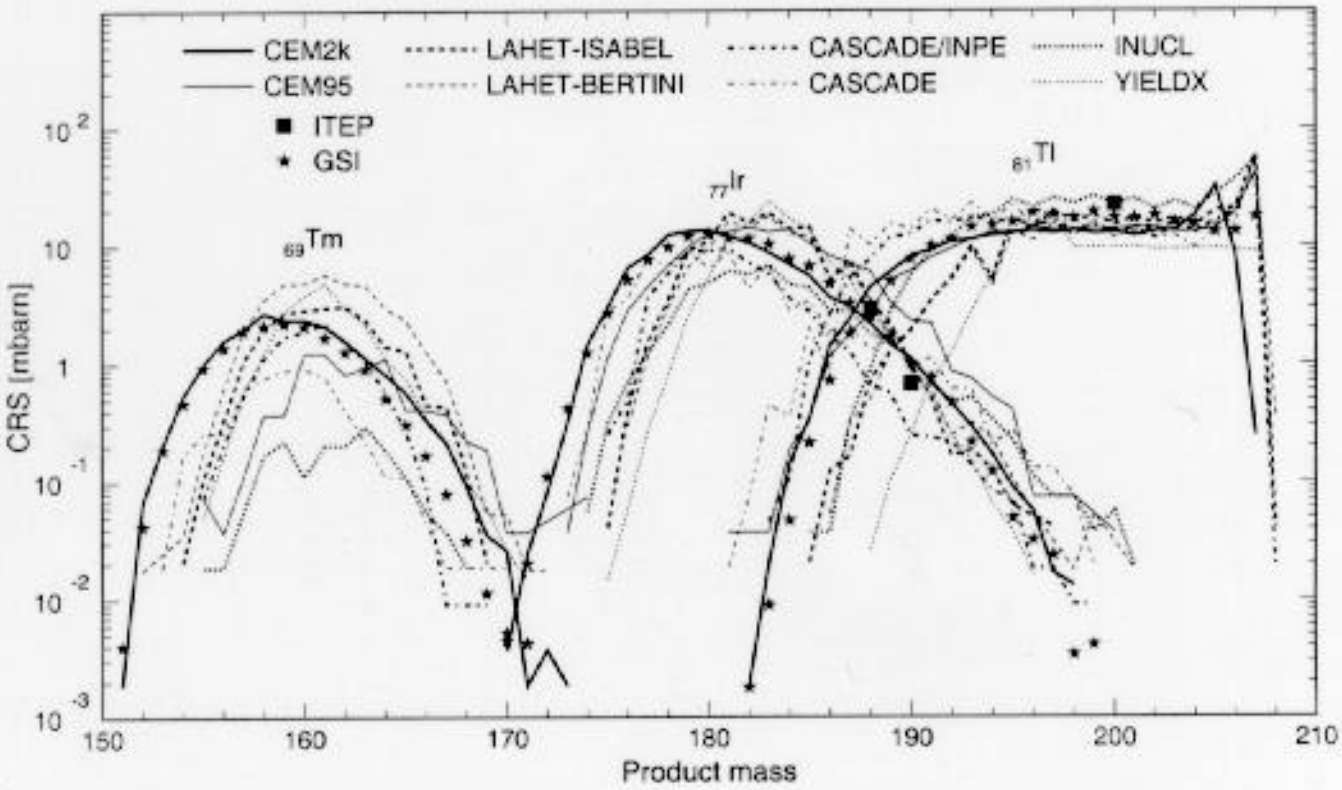

Figure 4: Isotopic mass distribution for independent products of Tm, Ir, and Tl isotopes. Black squares are ITEP measurements [16], while filled stars show GSI data obtained in reverse kinematics [6]. Results from different codes are marked as: CEM2k - our results, CEM95 - [2], LAHET-ISABEL - [10], LAHET-Bertini - [10], CASCADE/INPE - [17], CASCADE - [18], INUCL - [19], and YIELDX - [12].

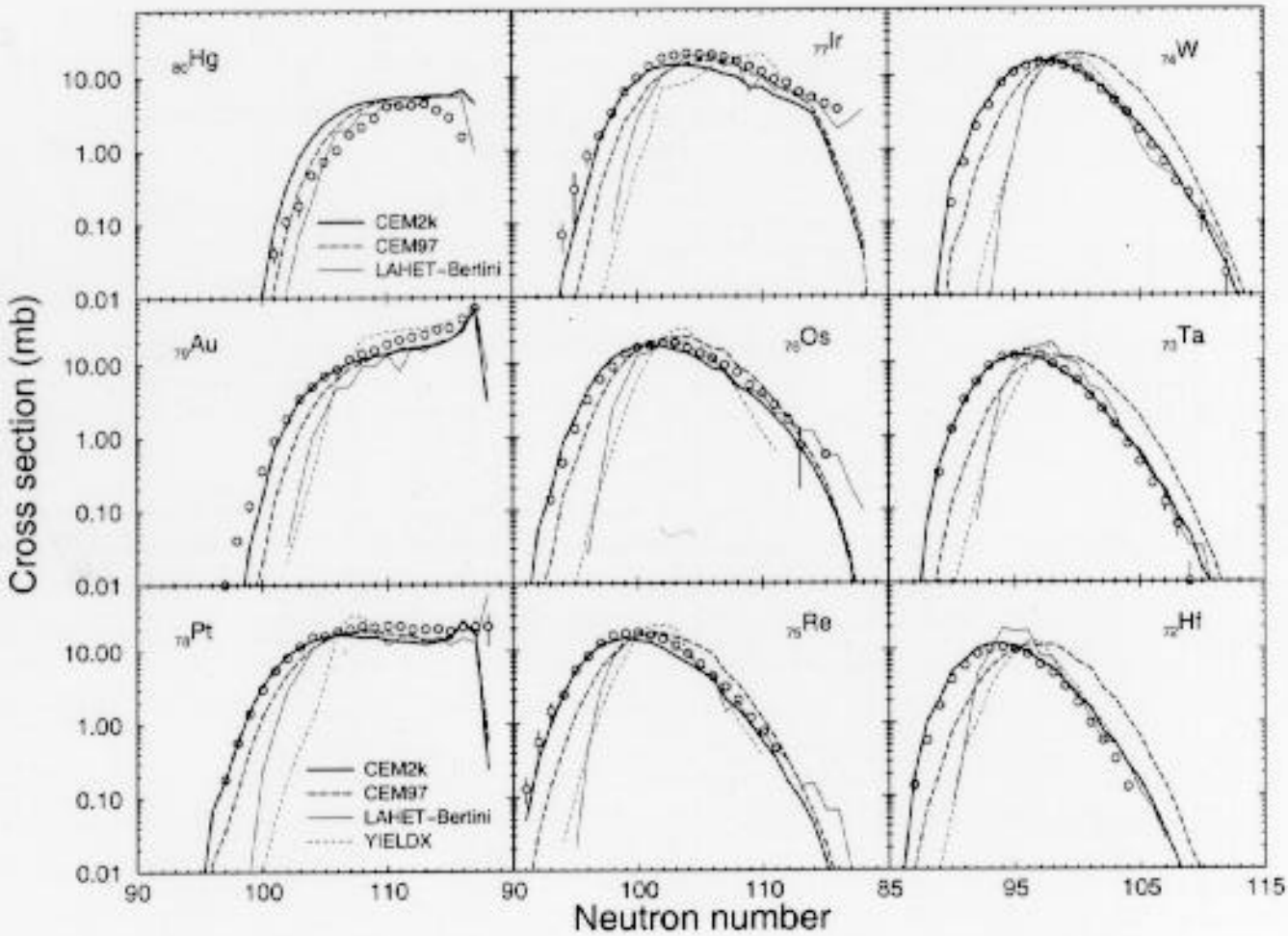

Figure 6: Isotopic distribution of the spallation residues produced in the reaction ^{197}Au + p at 800 A MeV from mercury to hafnium. Opened circles are the GSI data [9], CEM2k (thick solid curves) and CEM97 (thick dashed curves) are our present calculations, LAHET-Bertini (thin solid curves) and YIELDX (thin dashed curves) are results of calculations form [9].

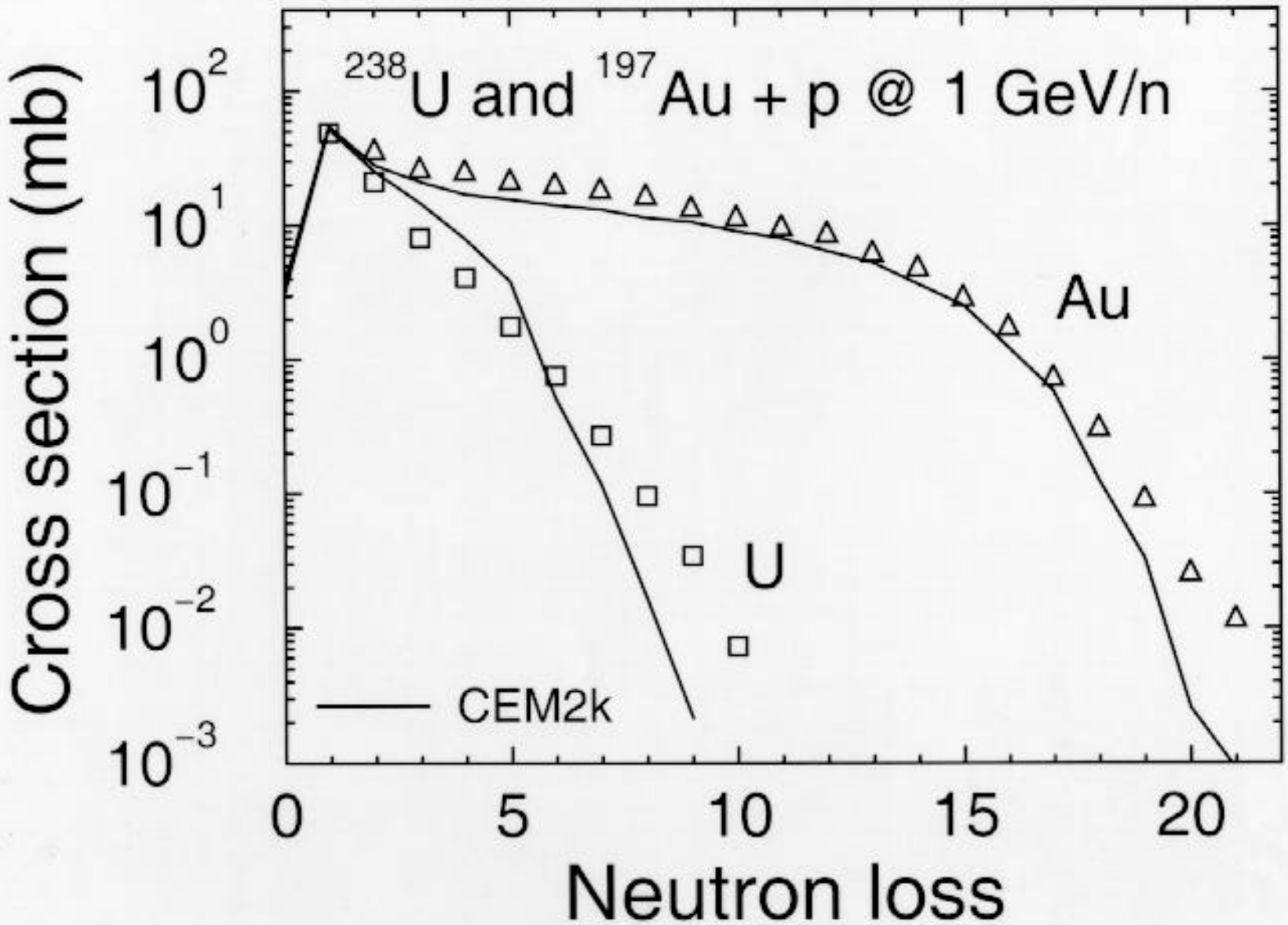
^{238}U and ^{197}Au + p @ 1 GeV/n
Cross section (mb)
10^{2}
10^{1}
10^{0}
10^{-1}
10^{-2}
10^{-3}
Au
U
CEM2k
0
5
10
15
20
Neutron loss

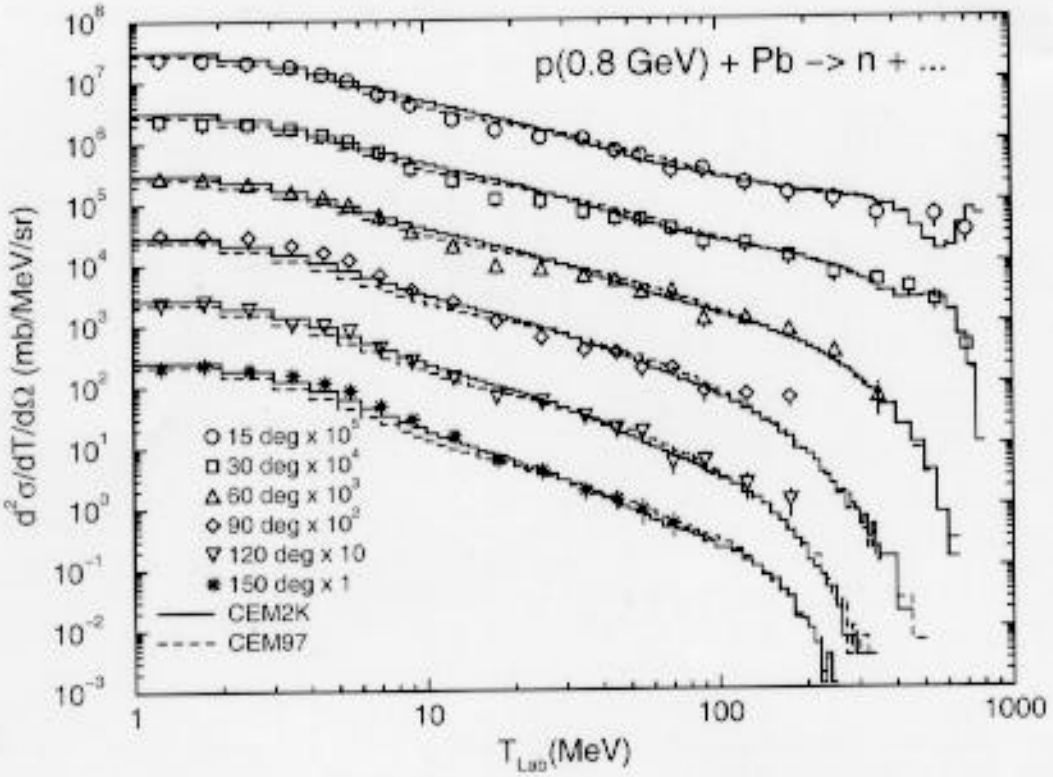
p(0.8 GeV) + Pb -> n + ...
15 deg x 10^5
30 deg x 10^4
60 deg x 10^3
90 deg x 10^2
120 deg x 10
150 deg x 1
CEM2K
CEM97
d^2σ/dT/dΩ (mb/MeV/sr)
T_Lab(MeV)

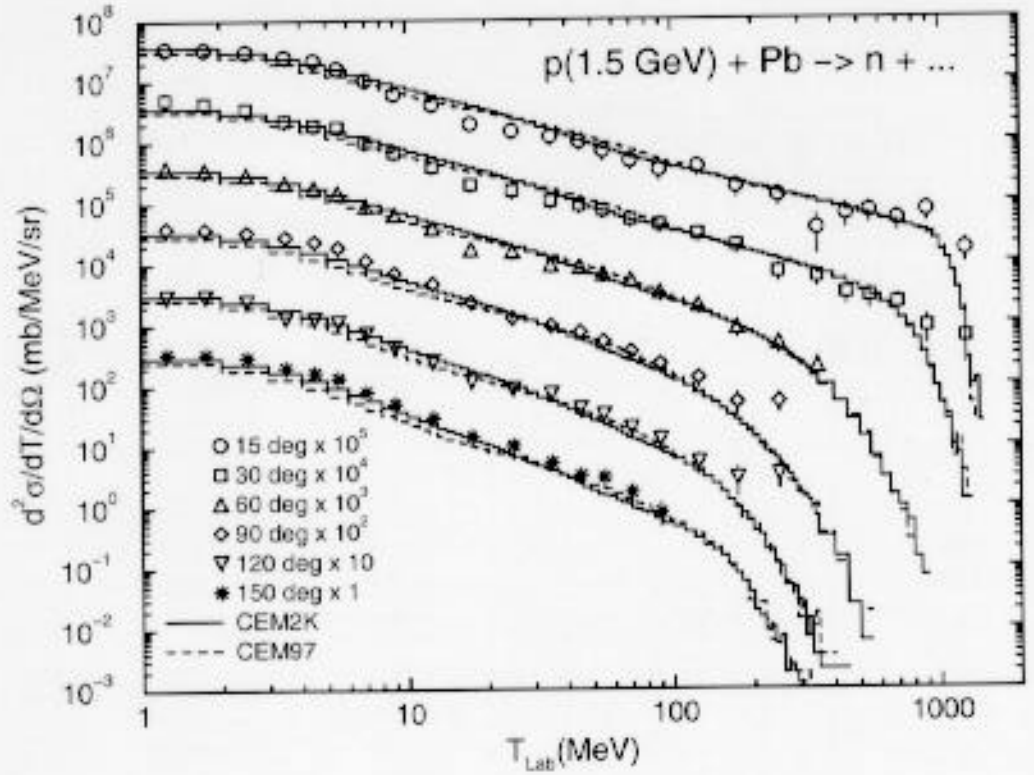
p(1.5 GeV) + Pb -> n + ...
15 deg x 10^5
30 deg x 10^4
60 deg x 10^3
90 deg x 10^2
120 deg x 10
150 deg x 1
CEM2K
CEM97
d^2σ/dT/dΩ (mb/MeV/sr)
T_Lab(MeV)

Table 1: Mean mass number, A, charge, Z, excitation energy, E^* (MeV), and angular momentum L ($\hbar$) of the compound nuclei formed after the preequilibrium stage of reactions calculated by different approaches as plotted in Fig. 2

Method	A	Z	E^*	L
CEM97 (plot a and b)	193.9	78.2	58.7	24.6
$\Gamma_\alpha \rightarrow 2\Gamma_\alpha$ (plot c)	193.4	78.0	58.3	24.8
Only $\Delta_n = +2$ (plot d)	196.4	78.6	86.4	24.1
No $\mathcal{P}$ (plot e)	191.0	77.5	65.0	21.3
CEM2k (plot f)	193.9	78.1	97.5	20.8